Journal of Sound and Vibration (2000) **230**(4), 809–824
doi:10.1006/jsvi.1999.2652, available online at http://www.idealibrary.com on IDEAL®

SOUND REFLECTION AND TRANSMISSION OF COMPLIANT PLATE-LIKE STRUCTURES BY A PLANE SOUND WAVE EXCITATION

G. R. LIU, C. CAI AND K. Y. LAM

Institute of High Performance Computing, 89-*B Science Park Drive* #01-05/08, *The Rutherford Singapore Science Park* 1, *Singapore* 118261, *Singapore*

(*Received* 15 *June* 1999, *and in final form* 14 *September* 1999)

The sound transmission and reflection by an infinite compliant plate-like structure immersed in fluids are analyzed using an exact method. A matrix formulation for the submerged plate with a stack of arbitrary number of anisotropic or isotropic layers, and subject to a plane sound wave excitation, is derived to obtain the transmission and reflection coefficients in the frequency domain. The coupling between the fluid and plate is taken into account in a rigorous manner. Several application examples are used to evaluate the effects of the thickness of the coating layer and base plate, the mutual position of layers, and the damping loss factors on the sound transmission and reflection. Results show that the coating layer attached to a steel base plate can effectively decrease the sound reflection by an average amount of about 6 dB above a frequency of 10 kHz when the coating layer of thickness 100 mm is on the incidence side.

1. INTRODUCTION

A compliant plate-like structure usually consists of elastic coating layers attached to a base plate, which may be of isotropy or anisotropy. The theoretical study of Koval [1], which provided the first model for noise transmission loss of composite constructions, was for an infinite monocoque cylindrical shell. In the analysis, Koval's mathematical model was based on the shell modal impedance. Roussos *et al.* [2] gave a report about the theoretical and experimental study of noise transmission through composite plates in the NASA Langley Research Centre on Ramakrishnan *et al.* [3] provided a theoretical model of finite element treatment of noise transmission through a stiffness panel into a closed cavity. They adopted the differential equation for mid-plane symmetrical laminated composite panels. Nayfeh *et al.* [4] reported a theoretical analysis based on an exact two-dimensional wave mechanics calculation of the amplitude of the reflected and transmitted partial waves in a liquid-coupled, arbitrarily in-plane oriented orthotropic plate. Arikan *et al.* [5] calculated the reflection coefficient of acoustic waves incident on a liquid–solid interface from the liquid side for a general anisotropic solid oriented direction. Liu *et al.* [6] investigated the interaction between the laminate and the water in a one-dimensional model and the effects of the laminate–water interaction on the wave fields in the laminate. Furthermore, Liu presented an exact matrix formulation for analyzing the response of anisotropic laminated plates subjected to line loads in a two-dimensional model [7].

Nayfeh [8] included a simple introduction of several salient contributions on interaction of waves and composite structures, such as "effective modulus techniques", "effective stiffness techniques" and "mixture techniques". As one of the effective techniques for the interaction of sound waves with the planar layered media, "matrix transfer technique" was applied [9–12]. The transfer matrix is constructed for a stack of arbitrary number of layers by extending the solution from one layer to the next while satisfying the appropriate interfacial continuity conditions. Based on the existing methods for analyzing the elastodynamic response of a plate, Liu *et al.* [7] grouped these methods into three categories: methods based on classic plate theories, numerical methods [13–20] and exact methods. In the exact methods, the equations of motion subjected to the boundary conditions are solved without any assumption. One distinguished advantage of the exact methods is the feasibility for computing responses at high frequencies.

The purpose of the current work is to analyze sound transmission and reflection of compliant structures immersed in fluids using an exact method. A plane acoustic wave is incident from the fluid on to the structure. The effects of the thickness of the coating layer and base plate, the mutual position of layers, and the damping loss factor, etc. on the acoustic response are evaluated. Results show that the outer coating layers have less sound reflection. A 100 mm thick elastomer layer facing the incident sound source can effectively decrease the sound reflection by an average amount of about 6 dB above a frequency of 10 kHz. There exists an optimal thickness of the coating layer with respect to a given base plate for minimum sound reflection in a specific frequency range.

2. FORMULATION

An infinite compliant plate-like structure made of N layers of arbitrary anisotropic materials separates the upper fluid from the lower fluid. To maintain generality, upper and lower fluids may be different as in Figure 1. h_n is the thickness of the nth layer. The origin of the local co-ordinate system is located on the bottom of each layer. θ and φ are the sound incident and azimuthal angles respectively (a list of nomenclature is given in Appendix A). If the azimuthal angle φ is zero, the incident sound wave insonifies the plate only in the x–z plane. All the derivations below are based on the assumption of a zero azimuthal angle. The formulation can be extended to the sound incidence with a non-zero azimuthal angle through an appropriate co-ordinate transformation as described in the last paragraph of section 2.4.

The incident plane sound wave can be expressed as

$$p^{in} = \bar{p}^{in}\, \mathrm{e}^{\mathrm{i}(k_{xw2}x - k_{zw2}z - \omega t)}, \tag{1}$$

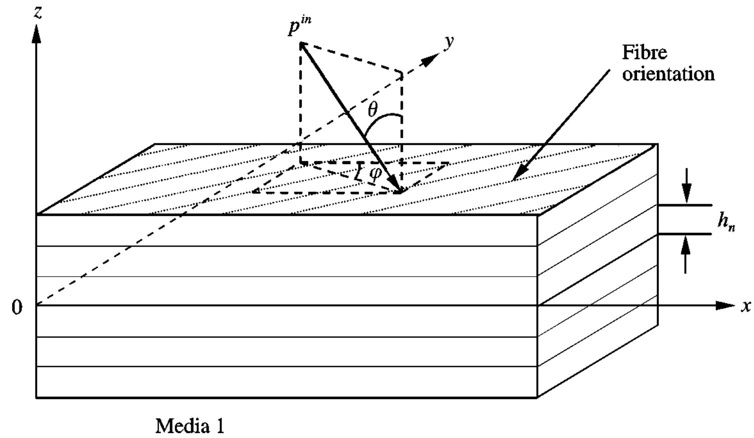

Figure 1. A sketch of physical model.

where $\bar{p}^{in}$ is the amplitude of the incident sound wave, $k_{xw2} = |\mathbf{k}_{w2}| \sin\theta$ and $k_{zw2} = |\mathbf{k}_{w2}| \cos\theta$, the two components of $\mathbf{k}_{w2}$ that are wave number vectors in the upper fluid. ω is the angular frequency, $\mathrm{i} = \sqrt{-1}$.

2.1. BASIC EQUATIONS FOR A LAYER IN THE PLATE

In order to simplify the formulation procedure, the following assumptions are introduced: (1) each layer lies in the x–y plane, (2) the interface between adjacent layers are perfectly bonded and (3) each layer has monoclinic properties if it is of anisotropy.

Within a layer, the motion is governed by the wave equation. In the case of absence of body force, the governing differential equation is expressed for the layer of the plate as [7]

$$\rho\ddot{\mathbf{U}} - \mathbf{L}^{\mathrm{T}}\mathbf{c}\mathbf{L}\mathbf{U} = 0, \tag{2}$$

where ρ is the mass density of the material of the layer, and $\mathbf{U}^{\mathrm{T}} = \{u \;\; v \;\; w\}$ in which u, v and w are the displacement components in x, y and z directions respectively. In equation (2), the dot indicates differentiation with respect to time, and the superscript "T" the transposition. The differential operator matrix $\mathbf{L}$ for the two-dimensional problem may be written as

$$\mathbf{L}^{\mathrm{T}} = \begin{bmatrix} \dfrac{\partial}{\partial x} & 0 & 0 & 0 & \dfrac{\partial}{\partial z} & 0 \\ 0 & 0 & 0 & \dfrac{\partial}{\partial z} & 0 & \dfrac{\partial}{\partial x} \\ 0 & 0 & \dfrac{\partial}{\partial z} & 0 & \dfrac{\partial}{\partial x} & 0 \end{bmatrix}. \tag{3}$$

The strain tensor $\varepsilon^{\mathrm{T}} = \{\varepsilon_{xx} \;\; \varepsilon_{yy} \;\; \varepsilon_{zz} \;\; \gamma_{yz} \;\; \gamma_{xz} \;\; \gamma_{xy}\}$ is obtained from

$$\varepsilon = \mathbf{L}\mathbf{U} \tag{4}$$

and the stress tensor $\sigma^{\mathrm{T}} = \{\sigma_{xx}\ \sigma_{yy}\ \sigma_{zz}\ \tau_{yz}\ \tau_{xz}\ \tau_{xy}\}$ is

$$\sigma = \mathbf{c}\varepsilon, \tag{5}$$

where $\mathbf{c} = (c_{ij})$, i, j = 1, …, 6 defines the matrix of 36 elastic constants for general anisotropic materials. It is known that only 21 constants exist for the most general anisotropic cases [21]. The effect of damping in materials is simulated by complex elastic modulus, namely, $E_{ii} = E'_{ii}(1 - \mathrm{i}\eta_e)$ and $G_{ij} = G'_{ii}(1 - \mathrm{i}\eta_g)$, where η_e and η_g are the longitudinal and shear loss factors. E'_{ii} and G'_{ij} are Young's and shear moduli without cosideration of damping effect respectively.

The operator matrix $\mathbf{L}$ in equation (2) can be rewritten as

$$\mathbf{L} = \mathbf{L}_x \frac{\partial}{\partial x} + \mathbf{L}_z \frac{\partial}{\partial z}, \tag{6}$$

where $\mathbf{L}_x$ and $\mathbf{L}_z$ can be obtained by inspection.

By using this definition of $\mathbf{L}$, the operator product $\mathbf{L}^{\mathrm{T}}\mathbf{c}\mathbf{L}$ in equation (2) becomes

$$\mathbf{L}^{\mathrm{T}}\mathbf{c}\mathbf{L} = \mathbf{D}_{xx} \frac{\partial^2}{\partial x^2} + 2\mathbf{D}_{xz} \frac{\partial^2}{\partial z \partial x} + \mathbf{D}_{zz} \frac{\partial^2}{\partial z^2}, \tag{7}$$

in which

$$\mathbf{D}_{xx} = \begin{bmatrix} c_{11} & c_{16} & c_{15} \\ & c_{66} & c_{56} \\ (sym) & & c_{55} \end{bmatrix}, \tag{8a}$$

$$\mathbf{D}_{xz} = \frac{1}{2} \begin{bmatrix} 2c_{15} & c_{14} + c_{56} & c_{13} + c_{55} \\ & 2c_{46} & c_{45} + c_{36} \\ (sym) & & 2c_{35} \end{bmatrix}, \tag{8b}$$

$$\mathbf{D}_{zz} = \begin{bmatrix} c_{55} & c_{45} & c_{35} \\ & c_{44} & c_{34} \\ (sym) & & c_{33} \end{bmatrix}. \tag{8c}$$

The stresses on a plane (z = constant) can be written as

$$\mathbf{R} = \{\tau_{xz}\ \tau_{yz}\ \sigma_{zz}\}^{\mathrm{T}} = \mathbf{L}_z^{\mathrm{T}}\mathbf{c}\mathbf{L}\mathbf{U}. \tag{9}$$

2.2. WAVE FIELD IN THE PLATE

Consider a harmonic wave field in the layer. The solution for equation (2) can be written in the form of

$$\mathbf{U} = \bar{\mathbf{U}}\mathbf{e}^{\mathrm{i}(k_x x + k_z z - \omega t)}, \tag{10}$$

where $\bar{\mathbf{U}}$ is the amplitude of the displacement, and k_x and k_z are the wave numbers in the layer with respect to directions x and z respectively. The substitution of equation (10) into equation (2) leads to the following equation:

$$[(\rho\omega^2\mathbf{I} - k_x^2\mathbf{D}_{xx}) - k_z(2k_x\mathbf{D}_{xz}) - k_z^2\mathbf{D}_{zz}]\bar{\mathbf{U}} = 0, \tag{11}$$

where $\mathbf{I}$ is the 3×3 identity matrix. Equation (11) can be changed to be the following standard eigenvalue equation in terms of k_z [22]:

$$\begin{bmatrix} 0 & \mathbf{I} \\ \mathbf{D}_{zz}^{-1}(\rho\omega^2\mathbf{I} - k_x^2\mathbf{D}_{xx}) & -2k_x\mathbf{D}_{zz}^{-1}\mathbf{D}_{xz} \end{bmatrix} \begin{Bmatrix} \bar{\mathbf{U}} \\ \mathbf{k}_z\bar{\mathbf{U}} \end{Bmatrix} - \mathbf{k}_z \begin{bmatrix} \mathbf{I} & 0 \\ 0 & \mathbf{I} \end{bmatrix} \begin{Bmatrix} \bar{\mathbf{U}} \\ k_z\bar{\mathbf{U}} \end{Bmatrix} = 0. \quad (12)$$

Equation (12) can be solved for given k_x and ω, and the six eigenvalues and the corresponding eigenvectors are obtained. Generally, the six eigenvalues and their eigenvectors are complex valued. Using the eigenvalues ζ_j and their eigenvectors $\mathbf{d}_j$, the displacement can be expressed as

$$\mathbf{U} = \mathbf{U}_z\mathbf{e}^{\mathrm{i}(k_x x - \omega t)}, \quad (13)$$

where $\mathbf{U}_z$ is only a function of co-ordinate z:

$$\mathbf{U}_z = \sum_{j=1}^{3} C_j^+\mathbf{d}_j^+\mathbf{e}^{\mathrm{i}\zeta_j^+ z} + \sum_{j=1}^{3} C_j^-\mathbf{d}_j^-\mathbf{e}^{\mathrm{i}\zeta_j^-(z-h)}, \quad (14)$$

where C_j^+ and C_j^- are constants to be determined from the boundary conditions on the lower and upper boundaries of the layer, and h is the thickness of the layer under consideration. The superscript " + " denotes waves propagating in the positive direction z (upward). The superscript " − " denotes wave propagating in the negative direction z (downward).

Equation (14) can be written in the matrix form

$$\mathbf{U}_z = \mathbf{V}^+\mathbf{E}^+(z)\mathbf{C}^+ + \mathbf{V}^-\mathbf{E}^-(z)\mathbf{C}^- = \{\mathbf{V}^+\mathbf{E}^+ \ \ \mathbf{V}^-\mathbf{E}^-\} \begin{Bmatrix} \mathbf{C}^+ \\ \mathbf{C}^- \end{Bmatrix}, \quad (15)$$

where

$$\mathbf{C}^+ = \{C_1^+ \ \ C_2^+ \ \ C_3^+\}^{\mathrm{T}}, \quad \mathbf{C}^- = \{C_1^- \ \ C_2^- \ \ C_3^-\}^{\mathrm{T}}, \quad (16)$$

$$\mathbf{V}^+ = \{\mathbf{d}_1^+ \ \ \mathbf{d}_2^+ \ \ \mathbf{d}_3^+\}, \quad \mathbf{V}^- = \{\mathbf{d}_1^- \ \ \mathbf{d}_2^- \ \ \mathbf{d}_3^-\}, \quad (17)$$

$$\mathbf{E}^+(z) = \mathrm{Diag}\{\mathbf{e}^{\mathrm{i}\zeta_1^+ z} \ \ \mathbf{e}^{\mathrm{i}\zeta_2^+ z} \ \ \mathbf{e}^{\mathrm{i}\zeta_3^+ z}\}, \quad \mathbf{E}^-(z) = \mathrm{Diag}\{\mathbf{e}^{\mathrm{i}\zeta_1^-(z-h)} \ \ \mathbf{e}^{\mathrm{i}\zeta_2^-(z-h)} \ \ \mathbf{e}^{\mathrm{i}\zeta_3^-(z-h)}\}. \quad (18)$$

Using equations (9), (13) and (6), we obtain

$$\mathbf{R} = \mathbf{R}_z\,\mathbf{e}^{\mathrm{i}(k_x x - \omega t)}, \quad (19)$$

where

$$\mathbf{R}_z = \mathrm{i}k_x\mathbf{D}_z\mathbf{U}_z + \mathbf{D}_{zz}\frac{\partial\mathbf{U}_z}{\partial z}, \quad \mathbf{D}_z = \begin{bmatrix} c_{51} & c_{56} & c_{55} \\ c_{41} & c_{46} & c_{45} \\ c_{31} & c_{36} & c_{35} \end{bmatrix}. \quad (20, 21)$$

Substituting equation (15) into equation (20), we can obtain

$$\mathbf{R}_z = \{\mathbf{P}^+\mathbf{E}^+ \ \ \mathbf{P}^-\mathbf{E}^-\} \begin{Bmatrix} \mathbf{C}^+ \\ \mathbf{C}^- \end{Bmatrix}, \quad (22)$$

where

$$\mathbf{P}^+ = \mathrm{i}k_x\mathbf{D}_z\mathbf{V}^+ + \mathbf{D}_{zz}\mathbf{V}_\zeta^+, \quad \mathbf{P}_z^- = \mathrm{i}k_x\mathbf{D}_z\mathbf{V}^- + \mathbf{D}_{zz}\mathbf{V}_\zeta^-, \quad (23)$$

$$\mathbf{V}_\zeta^+ = \{\mathrm{i}\zeta_1^+\mathbf{d}_1^+ \ \ \mathrm{i}\zeta_2^+\mathbf{d}_2^+ \ \ \mathrm{i}\zeta_3^+\mathbf{d}_3^+\}, \quad \mathbf{V}_\zeta^- = \{\mathrm{i}\zeta_1^-\mathbf{d}_1^- \ \ \mathrm{i}\zeta_2^-\mathbf{d}_2^- \ \ \mathrm{i}\zeta_3^-\mathbf{d}_3^-\}. \quad (24)$$

2.3. WAVE FIELD IN THE FLUID

There exist two kinds of plane sound waves in the upper fluid. One is the incident sound wave and the other is the sound wave reflected or radiated by the plate. The former can be expressed as equation (1) and the latter as

$$p^{re} = \bar{p}^{re}\mathbf{e}^{\mathrm{i}(k_{xw2}x + k_{zw2}z - \omega t)}. \tag{25}$$

The particle velocities caused by the sound waves are in the direction of z

$$v^{in} = -\frac{k_{zw2}}{\omega\rho_{w2}}p^{in}, \quad v^{re} = \frac{k_{zw2}}{\omega\rho_{w2}}p^{re}. \tag{26}$$

Considering the boundary conditions in the upper fluid, it is noted that the fluid goes to infinity in the positive z direction. The radiation condition, which states that waves are up going towards infinity, must therefore be satisfied.

Similarly, there exists only a plane sound wave in the lower fluid, assuming that the fluid goes to infinity in the negative z direction as well. The transmitted plane wave can be expressed as

$$p^{tr} = \bar{p}^{tr}\,\mathbf{e}^{\mathrm{i}(k_{xw1}x - k_{zw1}z - \omega t)}, \quad v^{tr} = -\frac{k_{zw1}}{\omega\rho_{w1}}p^{tr}, \tag{27, 28}$$

where k_{zw1} is the z direction component of the wave number vector $\mathbf{k}_{w1}$, and ρ_{w1} the density in the lower fluid.

2.4. INTERACTION BETWEEN THE PLATE AND THE FLUID

Based on Snell's law, the x components of the wave vectors of incident, reflected and transmitted longitudinal and shear modes should be the same. The fluids are assumed to be isotropic, non-viscous and have no resistance to shear deformation. Therefore, continuity of velocities and stresses requires ω and k_x to be the same in all layers and in the upper and lower fluids. Three coupling and boundary conditions are

(1) on the interfaces between the layers of plate

$$\mathbf{R}_n^U = \mathbf{R}_{n+1}^L, \mathbf{U}_n^U = \mathbf{U}_{n+1}^L, \quad 1 \leqslant n \leqslant (N-1), \tag{29a}$$

where superscripts "U" and "L" stand for the upper and lower surfaces of the layer respectively.

(2) on the interface between the upper fluid and the plate

$$\dot{w}_N^U = (v_z^{in} + v_z^{re}), \quad \sigma_{zz,N}^U = -(p^{in} + p^{re}), \quad \tau_{xz,N}^U = 0, \quad \tau_{yz,N}^U = 0, \tag{29b}$$

where $\dot{w}_N^U$ is the velocity in the z direction on the upper surface of layer N.

(3) on the interface between the lower fluid and the plate

$$\dot{w}_1^L = v_z^{tr}, \quad \sigma_{zz,1}^L = -p^{tr}, \quad \tau_{xz,1}^L = 0, \quad \tau_{yz,1}^L = 0, \tag{29c}$$

where $\dot{w}_1^L$ is the velocity in the z direction on the lower surface of layer 1.

Satisfaction of equation (29) leads to

$$\mathbf{AC} = \mathbf{T}, \tag{30}$$

where

$$\mathbf{T} = \{0 \ \ 0 \ \ \cdots \ \ 0 \ \ -2\bar{p}^{in}\}^{\mathrm{T}}_{6N \times 1}, \tag{31}$$

and **C** consists of the constant vectors for all the layers.

$$\mathbf{C} = \{\mathbf{C}_1^+ \ \ \mathbf{C}_1^- \ \ \mathbf{C}_2^+ \ \ \mathbf{C}_2^- \ \ \cdots \ \ \mathbf{C}_N^+ \ \ \mathbf{C}_N^-\}^{\mathrm{T}}_{6N \times 1}. \tag{32}$$

There will be six dependent equations for each internal interface between the layers based on the continuity conditions. There are only three independent equations for the lowermost or uppermost surface of the plate. Therefore, there are $6 \times N$ equations for N layers.

The matrix **A** is given by

$$\mathbf{A} = \begin{bmatrix} \mathbf{Q}_1^+ & \mathbf{Q}_1^-\mathbf{E}_1^{L-} & 0 & 0 & 0 & 0 & 0 & \cdots & 0 \\ \mathbf{V}_1^+\mathbf{E}_1^{U+} & \mathbf{V}_1^- & -\mathbf{V}_2^+ & -\mathbf{V}_2^-\mathbf{E}_2^{L-} & 0 & 0 & 0 & \cdots & 0 \\ \mathbf{P}_1^+\mathbf{E}_1^{U+} & \mathbf{P}_1^- & -\mathbf{P}_2^+ & -\mathbf{P}_2^-\mathbf{E}_2^{L-} & 0 & 0 & 0 & \cdots & 0 \\ 0 & 0 & \mathbf{V}_2^+\mathbf{E}_2^{U+} & \mathbf{V}_2^- & -\mathbf{V}_3^+ & -\mathbf{V}_3^-\mathbf{E}_3^{L-} & 0 & \cdots & 0 \\ 0 & 0 & \mathbf{P}_2^+\mathbf{E}_2^{U+} & \mathbf{P}_2^- & -\mathbf{P}_3^+ & -\mathbf{P}_3^-\mathbf{E}_3^{L-} & 0 & \cdots & 0 \\ \vdots & \vdots & \cdots & \ddots & \ddots & \ddots & \vdots & \cdots & \vdots \\ 0 & 0 & \cdots & 0 & 0 & 0 & 0 & \mathbf{Q}_N^+\mathbf{E}_N^{U+} & \mathbf{Q}_N^- \end{bmatrix}_{6N \times 6N} \tag{33}$$

where

$$\mathbf{E}_n^{U+} = \mathrm{Diag}\{\mathbf{e}^{\mathrm{i}\zeta_1^+ h_n} \ \ \mathbf{e}^{\mathrm{i}\zeta_2^+ h_n} \ \ \mathbf{e}^{\mathrm{i}\zeta_3^+ h_n}\}, \quad \mathbf{E}_n^{L-} = \mathrm{Diag}\{\mathbf{e}^{-\mathrm{i}\zeta_1^- h_n} \ \ \mathbf{e}^{-\mathrm{i}\zeta_2^- h_n} \ \ \mathbf{e}^{-\mathrm{i}\zeta_3^- h_n}\}$$
$$(n = 1, 2, \ldots, N), \tag{34}$$

$$\mathbf{Q}_1^+ = \begin{bmatrix} P^+_{1,11} & P^+_{1,12} & P^+_{1,13} \\ P_{1,21} & P_{1,22} & P_{1,23} \\ P^+_{1,31} + \mathbf{i}r_1 V^+_{1,31} & P^+_{1,32} + \mathbf{i}r_1 V^+_{1,32} & P^+_{1,33} + \mathbf{i}r_1 V^+_{1,33} \end{bmatrix}, \tag{35}$$

$$\mathbf{Q}_1^- = \begin{bmatrix} P^-_{1,11} & P^-_{1,12} & P^-_{1,13} \\ P^-_{1,21} & P^-_{1,22} & P^-_{1,23} \\ P^-_{1,31} + \mathbf{i}r_1 V^-_{1,31} & P^-_{1,32} + \mathbf{i}r_1 V^-_{1,32} & P^-_{1,33} + \mathbf{i}r_1 V^-_{1,33} \end{bmatrix}, \tag{36}$$

$$\mathbf{Q}_N^+ = \begin{bmatrix} P^+_{N,11} & P^+_{N,12} & P^+_{N,13} \\ P^+_{N,21} & P^+_{N,22} & P^+_{N,23} \\ P^+_{N,31} - \mathbf{i}r_2 V^+_{N,31} & P^+_{N,32} - \mathbf{i}r_2 V^+_{N,32} & P^+_{N,33} - \mathbf{i}r_2 V^+_{N,33} \end{bmatrix}, \tag{37}$$

$$\mathbf{Q}_N^- = \begin{bmatrix} P^-_{N,11} & P^-_{N,12} & P^-_{N,13} \\ P^-_{N,21} & P^-_{N,22} & P^-_{N,23} \\ P^-_{N,31} - \mathbf{i}r_2 V^-_{N,31} & P^-_{N,32} - \mathbf{i}r_2 V^-_{N,32} & P^-_{N,33} - \mathbf{i}r_2 V^-_{N,33} \end{bmatrix} \tag{38}$$

in which $P^+_{n,ij}$, $P^-_{n,ij}$, $V^+_{n,ij}$ and $V^-_{n,ij}$ are the elements of matrices $\mathbf{P}^+_n$, $\mathbf{P}^-_n$ $\mathbf{V}^+_n$ and $\mathbf{V}^-_n$ for layer n respectively. And

$$r_1 = \rho_{w1} \frac{\omega^2}{k_{zw1}}, \quad r_2 = \rho_{w2} \frac{\omega^2}{k_{zw2}}. \tag{39}$$

By solving equation (30), vector **C** can be obtained. Therefore, the displacements (or velocities) and stresses in each layer can be obtained by equations (13) and (19).

The reflected sound pressure in the upper fluid can be obtained by the normal velocity continuity conditions. The reflection coefficient β_{re} is given by

$$\beta_{re} = \frac{\bar{p}^{re}}{\bar{p}^{in}} = \left| 1 + \frac{\omega \rho_{w2}}{k_{zw2}} \frac{\dot{w}^U_N}{\bar{p}^{in}} \right|. \tag{40}$$

The transmitted pressure in the lower fluid can also be obtained by the normal velocity continuity conditions, and the transmission coefficient β_T is given by

$$\beta_t = \frac{\bar{p}^{tr}}{\bar{p}^{in}} = \left| -\frac{\omega \rho_{w1}}{k_{zw1}} \frac{\dot{w}^U_1}{\bar{p}^{in}} \right|. \tag{41}$$

When the plane wave reflection and transmission coefficients are indicated in dB, they are $20 \log_{10}(|\beta_{re}|)$ and $20 \log_{10} (|1\beta_t|)$ respectively. The latter is also called the transmission loss of the plate.

It is noted that the appropriate co-ordinate transformation is needed if the incident sound wave has an azimuthal angle φ with respect to plane x–z. The ply orientation of all anisotropic layers should be added to the aximuthal angle φ. It is also noted that **T** in equation (31) is only a result of certain mathematical derivation. The effect of the angle of incident pressure on the response of the plate is taken into account both on the left-hand side of equation (30) via the application of Snell's law and in the amplitude of incident normal particle velocity.

3. APPLICATION EXAMPLES

The formulation above is applied to several application examples in order to analyze sound transmission and reflection of compliant plate-like structures by a plane sound wave excitation. The three configurations are shown in Figure 2 and 3. Unless otherwise specified, the geometrical parameters are listed in Table 1. The results are considered for the frequency range of 0–50 kHz, which is typical of underwater acoustic applications. Default values of angles of incidence are taken as $\theta = 30^\circ$ and $\varphi = 0^\circ$.

First, two-layer plates consisting of a base plate and a coating layer (above and below the base plate respectively) are studied. The effect of geometrical combinations and thickness variations of these two layers on the acoustic performance is investigated. Second, the sandwich plates with two different soft fillers are evaluated. Filler A is of isotropy and filler B is of anisotropy.

Figure 4 shows the sound transmission and reflection of the structure with the thickness variance of coating layer. Parameter $t_c = 0$ in Figures 4–7 means that the coating layer does not exist. The upper fluid is water and the lower is air. The effect

Figure 2. The geometric schematic of two-layer plates: (a) A plate with a coating layer above; (b) A plate with a coating layer below.

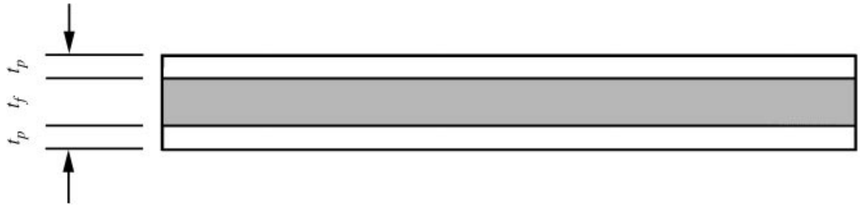

Figure 3. The geometric schematic of a sandwich plate.

TABLE 1

Material properties (EI)

No.	Material constants	E_1 (GPa)	E_2 (GPa)	G_{12} (GPa)	G_{23} (GPa)	v_{12}	v_{23}	ρ (kg/m^3)	η ($\eta_e = \eta_g$)	t (m)
1	Base plate	210	210	80·153	80·153	0·31	0·31	7800	0·002	0·01
	Coating layer	3·3 ∗ E-1	3·3 ∗ E-1	0·1107	0·1107	0·49	0·49	1200	0·8	0·01
2	Base plate	210	210	80·153	80·153	0·31	0·31	7800	0·002	0·005
	Filler A	3·3 ∗ E-1	3·3 ∗ E-1	0·1107	0·1107	0·49	0·49	1200	0·8	0·01
	Filler B	81·0	1·7	0·53	0·51	0·008	0·4	1420	0·2	0·01

of impedance mismatch due to air below causes the full sound reflection when no coating layer exists. The external-coating layer attached onto the base plate increases transmission loss and decreases sound reflection coefficient of the structure effectively. The compliant structure will have more than 4 dB reduction of reflection coefficient in the high-frequency range (20 kHz above) when covered with an elastomer layer of 5 mm thickness. With the increase of thickness of the coating layer, the reduction effect of sound reflection coefficient shifts to the lower-frequency range. However, the reduction effect will become worse with an increase in thickness in the high frequency. A 100 mm thick elastomer layer

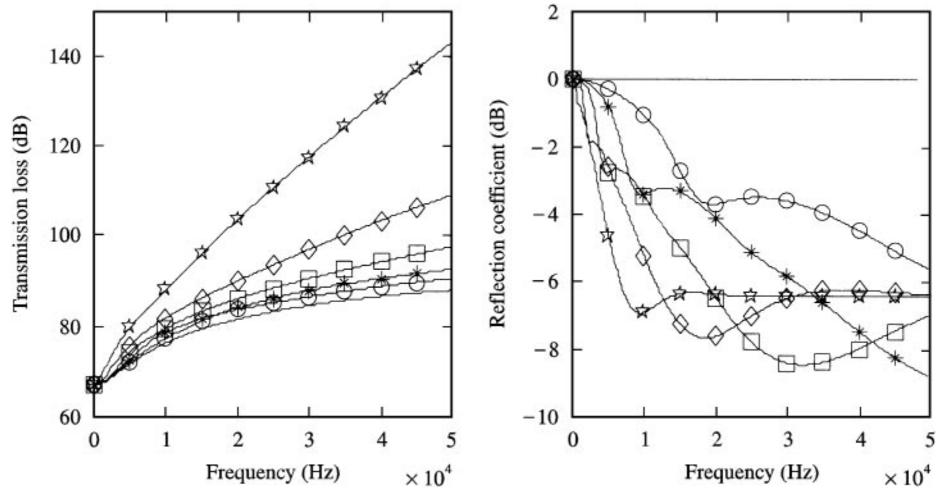

Figure 4. Transmission loss and reflection coefficients with various thickness of coating layer for coating layer above: ——, $t_c = 0$; –☆–☆–, $t_c = 0{\cdot}005$ m; –☆–☆–, $t_c = 0{\cdot}01$ m; –□–□–, $t_c = 0{\cdot}02$ m; –◇–◇–, $t_c = 0{\cdot}04$ m; –☆–☆–, $t_c = 0{\cdot}1$ m. ($t_p = 0{\cdot}01$ m, water–air).

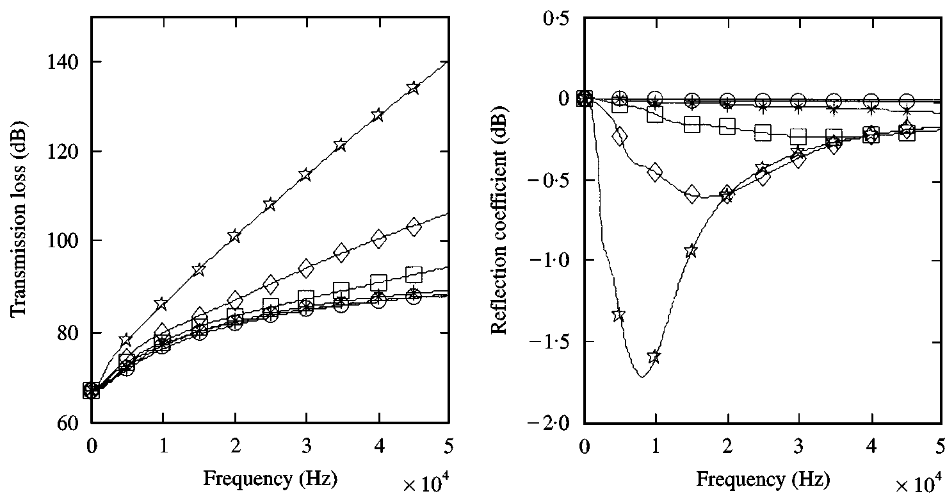

Figure 5. Transmission loss and reflection coefficients with various thickness of coating layer for coating layer below: ——, $t_c = 0$; –○–○–, $t_c = 0{\cdot}005$ m; –☆–☆–, $t_c = 0{\cdot}01$ m; –□–□–, $t_c = 0{\cdot}02$ m; –◇–◇–, $t_c = 0{\cdot}04$ m; –☆–☆–, $t_c = 0{\cdot}1$ m. ($t_p = 0{\cdot}01$ m, water–air).

attached to a base plate will decrease the sound reflection by an average amount of about 6 dB with frequencies of above 10 kHz.

Surface-attached coating layers are susceptible to damage inflicted by contact with surrounding objects. Hence, the case of a coating layer below the base plate is also considered as shown in Figure 5. The reduction of reflection coefficient is about $0 \sim -2$ dB, much smaller compared to the previous case. Meanwhile, the transmission loss in the case is also less than one when the coating layer faces the incident sound directly.

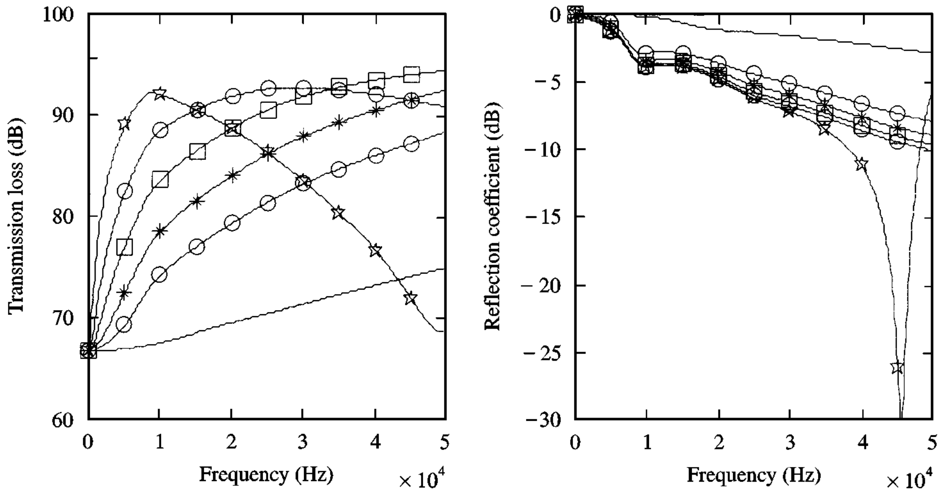

Figure 6. Transmission loss and reflection coefficients with various thickness of base plate for coating layer above: ——, $t_p = 0$; –○–○–, $t_c = 0{\cdot}005$ m; –☆–☆–, $t_p = 0{\cdot}01$ m; –□–□–, $t_p = 0{\cdot}02$ m; –◇–◇–, $t_p = 0{\cdot}04$ m; –☆–☆–, $t_p = 0{\cdot}1$ m. ($t_c = 0{\cdot}01$ m, water–air).

The effects of thickness change of the base plate on sound transmission and reflection coefficient are shown in Figure 6. Except in two cases, i.e., very thick base plate ($t_p = 100$ mm) and no base plate at all, varying thickness of the base plate does not affect the reduction of reflection coefficient obviously in most of the frequency range. The transmission loss of compliant structure will benefit from the increase of thickness of the base plate. It can be explained by the mass law.

When the coating layer is attached to the lower surface of base plate, the thickness change of the base plate almost does not affect the reflection coefficient except in the cases of very thick base plate and no base plate. The results are shown in Figure 7. It is noted in Figures 6 and 7 that the transmission loss for $t_p = 100$ mm decreases when the frequency is increased. This is because the critical frequency of the structure is shifted down to the analysis frequency range 0–50 kHz when the thickness of the base plate reaches 100 mm.

The effect of upper and lower fluid on sound transmission loss and reflection coefficient is shown in Figure 8. When air is on the incidence side, the sound reflection coefficient is the same regardless of what kind of fluid exists on the other side of the base plate. The impedance mismatch of air and compliant structure determines the almost full reflection characteristic. It corresponds to the case in which the incident sound impinges on a "hard" boundary. However, the transmission loss for air to water differs obviously from the one for air to air. The strong coupling between the compliant structure and the lower fluid reduces the transmission loss of the compliant structure.

When water is on the incidence side, the reflection coefficients tend to be the same in the high frequencies but differ in the low-frequency range. The water to water case has a big reduction of reflection coefficient in the low frequencies.

The results in Figure 8 also show that the coating layer attached on to a base plate does not function in the reduction of sound reflection in the case where air is

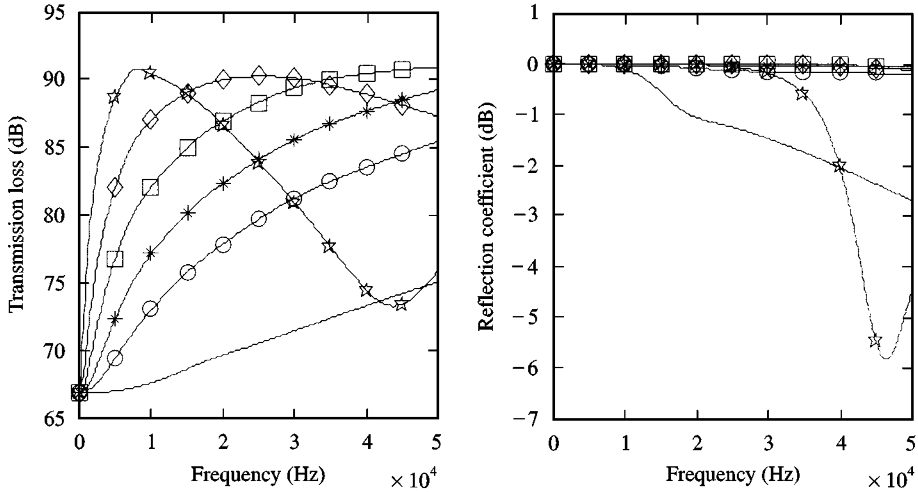

Figure 7. Transmission loss and reflection coefficients with various thickness of base plate for coating layer below: ——, $t_p = 0$; –○–○–, $t_p = 0{\cdot}005$ m; –☆–☆–, $t_p = 0{\cdot}01$ m; –□–□–, $t_p = 0{\cdot}02$ m; –◇–◇–, $t_p = 0{\cdot}04$ m; –☆–☆–, $t_p = 0{\cdot}1$ m. ($t_c = 0{\cdot}01$ m, water–air).

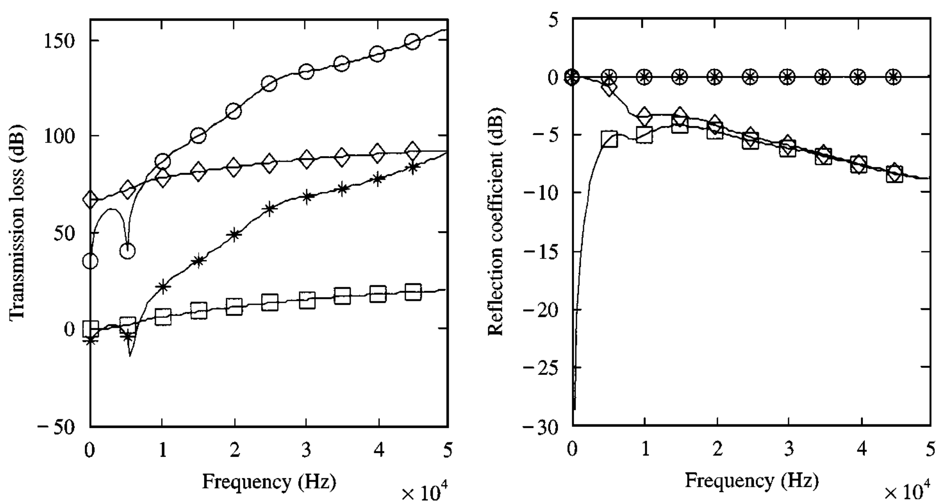

Figure 8. Transmission loss and reflection coefficients with different mediums for coating layer above. –○–○–, Air–air; –□–□–, Water–water; –☆–☆–, Air–water; –◇–◇–, Water–air. ($t_c = t_p = 0{\cdot}01$ m).

on the incidence side. It works only in the case where water is on the incidence side: water to air.

It is worth noting that the coating cover comes into effect only when it has a non-zero loss factor even in the water-to-air case. The loss factor for the coating layer plays an important role in reducing sound reflection and sound transmission as shown in Figure 9. A maximum loss factor may not result in a maximum reduction of sound reflection in a whole frequency range. It means that there exists

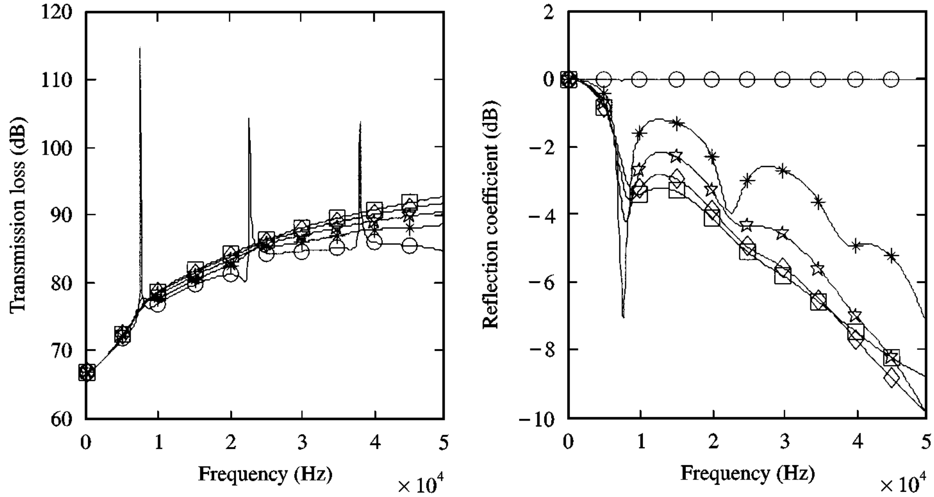

Figure 9. Transmission loss and reflection coefficients with different damping factors for coating layer above: −○−○−, $\eta = 0$; −☆−☆−, $\eta = 0{\cdot}2$; −☆−☆−, $\eta = 0{\cdot}4$; −◇−◇−, $\eta = 0{\cdot}6$. −□−□−, $\eta = 0{\cdot}8$; ($t_c = t_p = 0{\cdot}1$ m, water–air).

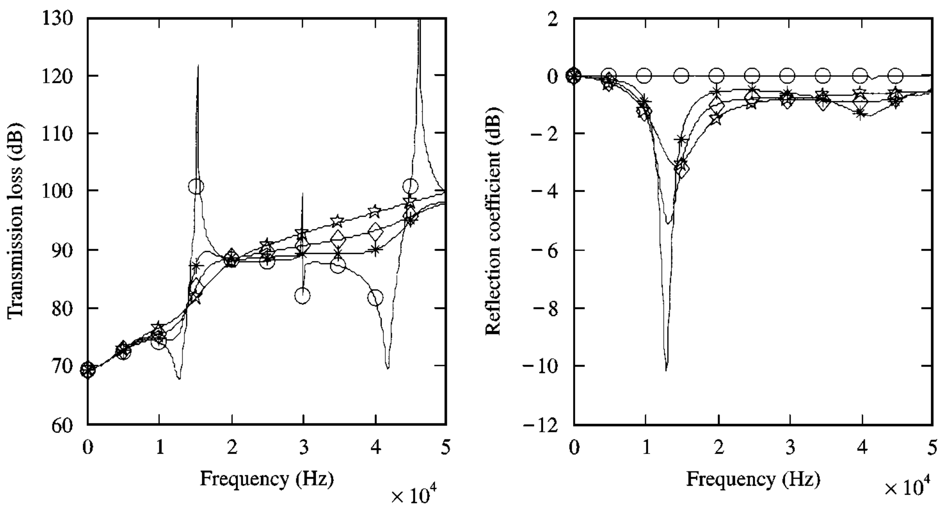

Figure 10. Transmission loss and reflection coefficients with different damping factors of filler A for the sandwich plate. −○−○−, $\eta = 0$; −☆−☆−, $\eta = 0{\cdot}2$; −◇−◇−, $\eta = 0{\cdot}4$; −☆−☆−, $\eta = 0{\cdot}8$. incident angle = 50° ($t_c = 0{\cdot}01$ m, $t_p = 0{\cdot}005$ m, water–air).

an optimum loss factor for a given structure. The "peaks" in the transmission loss curves in Figure 9 correspond to the shear waveguide behaviour in the coating cover. The increase in the coating damping loss will result in the reduction of the amplitudes of these "peaks".

Figure 10 introduces a sandwich plate, which divides the previous base plate into two surface plates, by sandwiching the coating layer as filler. The sandwich plate can protect the coating layer from damage more efficiently. Compared to Figure 5,

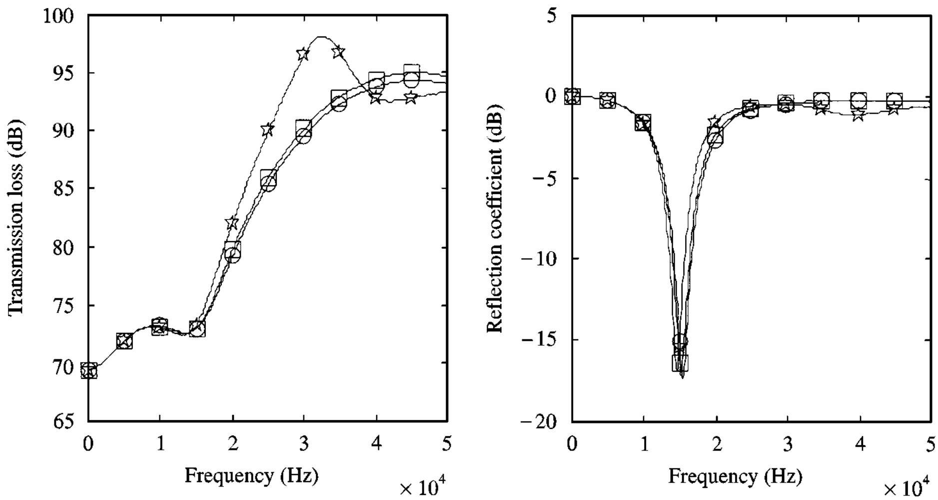

Figure 11. Transmission loss and reflection coefficients with different azimuthal angles for the sandwich plate (filler B): –○–○–, 0°; –□–□–, 45°; –☆–☆–, 90°; incident angle = 50° (t_c = 0·01 m, t_p = 0·005 m, water–air).

the sandwich plate has a bigger reduction of sound reflection. Figure 10 also indicates that a big loss factor of the filler may not result in a big reduction of sound reflection in a whole frequency range. The damping effect can smooth the transmission curve obviously. That means that the damping of the filler may affect the transmission loss in the coincidence region where the acoustic wavenumber in the upper fluid is equal to either the shear or longitudinal resonant wavenumber of the elastomer filler.

As we know, the azimuthal angle of incidence φ has no effect on the sound transmission and reflection for structures with isotropic properties. However, the angle φ has an effect on the sound transmission and reflection for structures with anisotropic properties. Figure 11 shows the effect of azimuthal angle on the sound transmission and reflection of the sandwich plate with filler B (anisotropic properties). This is because there are large differences in the Young's modulus in directions of x and y. The accoustic features, which are unique to anisotropic solids, will be investigated in future papers.

4. CONCLUSIONS

The transmission and reflection coefficients from an infinite compliant plate-like structure submerged in the fluids are investigated using an exact method. In the formulation, the coupling between the fluid and laminate is taken into account in a rigorous manner. With the formulation presented, the sound transmission and reflection by one two-layer plate and one sandwich plate are calculated. From these application examples, the following conclusions can be drawn. The reduction of reflection coefficient is sensitive to the existence of a coating layer. The compliant structure with a coating layer facing incident sound has a better reduction effect on sound reflection coefficient than an coating layer facing non-incidence side. The increase in coating thickness will improve the reduction effect in the low-frequency range but will lose the effect in the given higher-frequency range. The thickness change of base plate has little effect on the reflection coefficient. The method presented can be widely applied to study and evaluate the acoustic properties of both isotropic and anisotropic multi-layer structures. It can be extended to carry out the dynamic response of elastic coating excited by the plane sound waves as well.

REFERENCES

1. L. R. Koval 1980 *Journal of Sound and Vibration* **71**, 523–530. Sound transmission into a laminated composite cylindrical shell.
2. L. A. Roussos, C. R. Powell, F. W. Grosveld and L. R. Koval 1984 *Journal of Aircraft* **21**, 528–535. Noise transmission characteristics of advanced composite structure materials.
3. J. V. Ramakrishnan and L. R. Koval 1987 *Journal of Sound and vibration* **112**, 433–446. A finite element model for sound transmission through laminated composite plates.
4. A. H. Nayfeh and D. E. Chimenti 1988 *Journal of Applied Mechanics* **55**, 863–870. Ultrasonic reflection from liquid-coupled orthtropic plates with application to fibrous composite.
5. O. Arikan, E. Telatar and A. Atalar 1989 *Journal of the Acoustical Society of America* **85**, 1–10. Reflection coefficient null of acoustic waves at a liquid-anisotropic solid interface.
6. G. R. Liu, K. Y. Lam and E. S. Chan 1996 *Shock and Vibration* **3**, 419–433. Stress waves in composite laminates excited by transverse plane shock waves.
7. G. R. Liu, K. Y. Lam and J. Tani 1995 *Mechanics of Composite Materials and Structures* **2**, 227–241. An exact method for analysing elastodynamic response of anisotropic laminates to line loads.
8. A. H. Nayfeh and D. E. Chimenti 1988 *Journal of the Acoustical Society of America* **83**, 1736–1743. Propagation of guided waves in fluid-coupled plates of fiber-reinforced composite.
9. A. H. Nayfeh and T. W. Taylor 1988 *Journal of the Acoustical Society of America* **84**, 2187–2191. Surface wave characteristics of fluid-loaded multilayered media.
10. G. R. Liu, J. Tani, K. Watanabe and T. Ohyoshi 1990 *ASME Journal of Applied Mechanics* **57**, 923–929. Lamb wave propagation in anisotropic laminates.
11. H. Zheng 1992 *Ph.D. Thesis*, *Shanghai Jiaotong University*. A study on the sound transmission loss characteristics and vibratory damping properties of elastic–viscoelastic layered damping panels.
12. E. A. Skelton and J. H. James 1992 *Journal of Sound and Vibration* **152**, 154–174. Acoustic of anisotropic planar layered media.
13. G. R. Liu, J. Tani, K. Watanabe and T. Ohyoshi 1990 *Wave Motion* **12**, 361–371. A semi-exact method for the propagation of harmonic waves in anisotropic laminated bars of rectangular cross section.
14. G. R. Liu, J. Tani, T. Ohyoshi and K. Watanabe 1991 *ASME Journal of Vibration and Acoustics* **113**, 279–285. Characteristic wave surfaces in anisotropic laminated plates.
15. G. R. Liu and J. Tani 1991 *Transactions of the Japan Society of Mechanical Engineers* **57**(A), 180–185. Characteristics of wave propagation in functionally gradient piezoelectric material plates and its response analysis, part 1: theory.
16. G. R. Liu and J. Tani 1992 *Transactions of the Japan Society of Mechanical Engineers* **58**(A), 504–507. SH surface waves in functionally gradient piezoelectric material plates.

17. G. R. Liu, J. D. Achenbach, J. O. Kim and Z. L. Li 1992 *Journal of the Acoustical Society of America* **92**, 2734–2740. A combined finite element method/boundary element method for $V(z)$ curves of anisotropic-layer/substrate configurations.
18. G. R. Liu and J. D. Achenbach 1994 *ASME Journal of Applied Mechanics* **61**, 270–277. A strip element method for stress analysis of anisotropic linearly elastic solids.
19. G. R. Liu and J. D. Achenbach 1995 *ASME Journal of Applied Mechanics* **62**, 607–613. A strip element method to analyze wave scattering by cracks in anisotropic laminated plates.
20. G. R. Liu, Z. C. Xi, K. Y. Lam and H. M. Shang *Journal of Applied Mechanics*. A strip element method for analyzing wave scattering by a crack in an immersed composite laminates (accepted).
21. R. M. Jones 1975 *Mechanics of Composite Materials*. Washington, DC: Scripta Book Company.
22. S. B. Dong 1977 *International Journal for Numerical Methods in Engineering* **11**, 247–267. A block-Stodola eigensolution techniques for large algebraic systems with non-symmetrical matrices.

APPENDIX: NOMENCALTURE

c_{ij}	matrix of elastic constants of current layer
c_{w1}	sound speed in lower fluid
c_{w2}	sound speed in upper fluid
E_{ij}	complex Young's modulus
G_{ij}	complex shear modulus
h_n	thickness of nth layer
i	$\sqrt{-1}$, unit imaginary number
k_x, k_z	wave number components in current layer in x and z directions
$\mathbf{k}_{w1}$	wave number vector in lower fluid
k_{zw1}	component of $\mathbf{k}_{w1}$ in z direction
$\mathbf{k}_{w2}$	wave number vector in upper fluid
k_{xw2}, k_{zw2}	two components of $\mathbf{k}_{w2}$ in x and z directions respectively
N	total number of layers
$\bar{p}^{in}$	amplitue of incident sound wave
$\bar{p}^{re}$	amplitude of reflected sound wave
$\bar{p}^{tr}$	amplitude of transmitted sound wave
$\mathbf{R}$	stress vector on a given plane ($\mathbf{z}$ = constant); $\mathbf{R} = \{\tau_{xz}\ \tau_{yz}\ \sigma_{zz}\}^{\mathrm{T}}$
t	time co-ordinate
u, v, w	displacement components in x, y and z directions respectively; $\mathbf{U}^{\mathrm{T}} = \{u\ v\ w\}$
v^{in}	particle velocity of incident sound wave in z direction
v^{re}	particle velocity of reflected sound wave in z direction
v^{tr}	particle velocity of transmitted sound wave in z direction
β_{re}	reflection coefficient
β_t	transmission coefficient
ε	strain tensor; $\varepsilon^{\mathrm{T}} = \{\varepsilon_{xx}\ \varepsilon_{yy}\ \varepsilon_{xz}\ \gamma_{yz}\ \gamma_{xz}\ \gamma_{xy}\}$
η_e, η_g	longitudinal and shear loss factors respectively
θ	incidence angle of incident sound wave
ρ	mass density of current layer material
ρ_{w1}, ρ_{w2}	mass densities of lower and upper fluids respectively
σ	stress tensor, $\sigma^{\mathrm{T}} = \{\sigma_{xx}\ \sigma_{yy}\ \sigma_{zz}\ \tau_{yz}\ \tau_{xz}\ \tau_{xy}\}$
φ	azimuthal angle of incident sound wave
ω	angular frequency of excitation